J Mater Sci: Mater Med (2009) 20:1971–1978
DOI 10.1007/s10856-009-3772-7

Preparation and characterization of biodegradable poly(D,L-lactide) and surface-modified bioactive glass composites as bone repair materials

Du Juan Zhang · Li Fang Zhang · Zuo Chun Xiong · Wei Bai · Cheng Dong Xiong

Received: 24 December 2008 / Accepted: 4 May 2009 / Published online: 18 May 2009

Abstract In order to improve filler dispersion and phase compatibility between poly(D,L-lactide) (PDLLA) and inorganic bioactive glass (BG) particles, and to enhance the mechanical properties of PDLLA/BG composites, the silane coupling agent 3-glycidoxypropyltrimethoxysilane (KH570) was used to modify the surface of BG particles (represented by KBG). The structure and properties of PDLLA/BG and PDLLA/KBG composites were investigated by mechanical property testing and scanning electron microscopy (SEM). This study demonstrated that the Guth and Gold models can be combined to predict the Young's modulus of the composites. The Pukanszky modulus showed that the interaction parameter B of PDLLA/KBG composites was higher than that of the PDLLA/BG, which indicates that there is a higher interfacial interaction between the PDLLA and KBG. The composites were incubated in simulated body fluid (SBF) at 37°C to study the in vitro degradation and bioactivity of the composites and to detect bone-like apatite formation on their surfaces.

1 Introduction

Synthetic bioresorbable polymers, particularly, poly(D,L-lactide) (PDLLA) and polyglycolic acid (PGA) and their copolymer poly(D,L-lactic acid-co-glycolic acid), have attracted considerable attention for their use as bone-repair materials [1–11]. A number of reports state that these materials have proven biocompatibility and complete bioresorbability, and hence, they can be used as bone substitute material [3–6]. Moreover, all these synthetic bioresorbable polymers can be very easily fabricated into complex structures [7, 8]. However, a number of problems have been encountered when these materials are used as bone repair materials since they release acidic degradation products that lead to inflammatory responses [9–11]. Other limitations of biodegradable polymers are that the mechanical strength of all these synthetic bioresorbable was lower than those of natural cortical bones and that they lack a bioactive function, in particular, with respect to bone repair applications. In addition, bone apposition or bonding is not possible on the polymer surface.

Bioceramics such as hydroxyapatite (HAP), tricalcium phosphate (TCP), and bioactive glass (BG) are another important group of biomaterials [12, 13]. BG can react with physiological fluids and form tenacious bonds with hard (and in some cases soft) tissues [13–17]. However, the main factor limiting its application in bone repair is its brittleness; therefore, it has been used in the form of particulates [18–21].

Autografts are most widely used by surgeons. These grafts contain viable cells such as bone marrow osteoprogenitor cells, a collagenous matrix, and non-collagenous extracellular growth and differentiating factors. Consequently, the autograft is the preeminent therapy for bone repair, because it has osteogenic, osteoconductive, and osteoinductive properties [22]. The autograft is chemically and structurally equivalent to the mineral phase in bone. The mechanical property is similar to the bone. The major disadvantages of autograft are donor site morbidity and limitations on the quantity of graft materials.

D. J. Zhang · L. F. Zhang · Z. C. Xiong · W. Bai · C. D. Xiong (✉)
Chengdu Institute of Organic Chemistry, Chinese Academy of Sciences, Chengdu 6 10041, China
e-mail: 1633xiong@163.com

D. J. Zhang · Z. C. Xiong · W. Bai
Graduate University of Chinese Academy of Sciences, Beijing 100039, China

Given the limitations of current of treatment options and the need for improved clinical outcomes, biomaterials used for bone repair should have the properties of both bioresorbability and bioactivity [21]. Introduction of a bioactive phase to a bioresorbable polymer imparts it bioactivity to the polymer and allows rapid exchange of protons in water with the alkali in the bioglass or ceramic, thereby providing a pH-buffering effect at the polymer surface and reducing the acidic degradation of the polymer. Combining the bioactive materials with biopolymers could produce materials with better bioactive and bioresorbable properties. However, such particles would aggregate in the matrix because of their incompatibility with the biopolymer [23]. The phase-separation phenomenon that results from this aggregation would then induce graft failure at the interface and thus cause deterioration of the mechanical properties of the composites. Hence, the surface modification of bioceramic particles should be performed using organic molecules [24–26]. BG is a class A bioactive material that exhibits both osteoinductive and osteoconductive properties [12, 13]. Thus, by combining BG and KBG with PDLLA, it is possible to develop composites with bioactive properties that are potentially beneficial in bone repair materials can be developed.

In this study, we investigated the possibility of using bioresorbable and bioactive composites of PDLLA/BG and PDLLA/KBG as bone repair materials. We studied the mechanical and bioactive properties of composites containing BG and KBG particles. We used a semiempirical equation developed by Pukanszky to determine the interfacial interaction between the polymer matrix and the inorganic particles. We describe the preparation, characterization, and in vitro degradation of PDLLA/BG and PDLLA/BG composites and present the preliminary results regarding their bioactivity in simulated body fluid (SBF) solution.

2 Materials and methods

2.1 Materials

Amorphous PDLLA with an inherent viscosity of 4.03 dl/g was provided by Sichuan Dikang Sci & Tech Pharmaceutical Co. Ltd. (Chengdu, China). We used 60S sol–gel bioglass (BG) powder with a mean particle size of 2–5 μm that contained 60% SiO_2, 34% CaO, and 6% P_2O_5 (in molar percent). We prepared 60S BG by the hydrolysis and polycondensation of tetraethylorthosilicate (TEOS), triethyl phosphate (TEP), and 2-methoxyethane calcium alkoxide [27]. The properties of BG particles formed were characterized by Fourier Transform infrared FTIR spectroscopy, X-ray diffraction (XRD) analysis, and X-ray photoelectron spectroscopy (XPS; Axis Ultra; Kratos Analytical Ltd., UK). The silane coupling agent 3-glycidoxypropyltrimethoxysilane (KH570) was provided by Sichuan University.

2.2 Surface modification of BG particles

Surface modification of the BG particles with KH570 was carried out in solution [28]. KH570 (0.5 wt%) was dissolved in 80 v% aqueous ethanol solution, and the pH was adjusted to 4.0 with HAc buffer. The BG particles were dispersed in the ethanol solution in a ratio of 20% (w/v). Subsequently, the KH570 solution was added to the BG slurry. The slurry was mixed for 3 h on a magnetic stirrer by refluxing at 100°C. The surface modification of the BG particles with KH570 was completed by drying the slurry for 4 h in a vacuum oven at 120°C. Next, the surface-modified BG particles were washed exhaustively with water to remove the unbound KH570. After centrifugation, the KH570-modified BG particles (KBG) were dried at 120°C. The particles were characterized by X-ray photoelectron spectroscopy (XPS), and the results indicated that their Si content had increased.

2.3 Preparation of the composites

The PDLLA granules were dissolved in acetone in an Erlenmeyer flask in order to obtain an initial polymer weight to solvent ratio of 5% (w/v). The polymer suspension was stirred to obtain a homogeneous polymer solution. Appropriate amounts of the BG and KBG particles were then added to the polymer solution to obtain different proportions of the weights of BG and KBG to that of the polymer. Subsequently, the mixture was sonicated for 30 min in an ultrasonic water bath to improve the dispersion of the BG particles in the polymer solution. Finally, the composites were deposited by adding a large amount of ethanol. The resulting composite powder was dried in vacuum at 25°C for 48 h in order to remove the remaining solvent. Dumbbell-shaped specimens with effective dimensions of 26 × 5 × 2 mm were prepared from the composites by compression-molding under a pressure of 10 MPa. The temperature for processing pure PDLLA, PDLLA/BG, and PDLLA/KBG was 180°C. These specimens were maintained at room temperature for 3 days before characterization.

2.4 Mechanical property and scanning electron microscopy (SEM) analysis

Tensile specimens of PDLLA/BG and PDLLA/KBG composites were tested using a universal testing machine (CMT4503; Shenzhen SANS Testing Machine Co. Ltd., China). The specimens were tested at 25°C by using a

crosshead speed of 2 mm/min. The tensile strength and modulus data were both obtained by averaging over five replicate specimens.

SEM was used to determine the homogeneity of the PDLLA/BG and PDLLA/KBG composite microstructures to assess the quality of the dispersion of BG and KBG in the PDLLA matrix. Samples were gold coated for 120 s at 20 mA and examined under a JSM-5900 (JSM; Japan) at an accelerating voltage of 10 kV.

2.5 In vitro bioactivity studies

In vitro bioactivity studies were performed using a standard SBF on the basis of the formulation and method developed by Kokubo et al. [15]; the inorganic ion concentration of this SBF is similar to that of human blood plasma. The SBF was prepared by dissolving appropriate amounts of chemical reagents such as NaCl, $NaHCO_3$, KCl, $K_2HPO_4 \cdot 3H_2O$, $MgCl_2 \cdot 6H_2O$, $CaCl_2 \cdot 2H_2O$, and Na_2SO_4 into deionized water. The pH of the SBF was adjusted to physiological pH (pH 7.4) by adding HCl and buffered by Tris (hydroxymethyl) aminomethane at 37°C.

Dry PDLLA/BG and PDLLA/KBG composites and PDLLA were immersed in SBF solution with a weight to volume ratio of 8×10^{-3} in clean polythene bottles that had been washed using deionized water. The bottles containing the samples immersed in SBF were placed inside an incubator at a controlled temperature of 37°C. After 7, 14, and 21 days, the samples were removed from the buffer and rinsed with deionized water to remove any soluble inorganic salt. The structural and morphological variations of the composite surface before and after soaking in SBF were analyzed by X-ray diffraction (XRD) using a Philips X'Pert diffractometer with CoKa radiation and by SEM analysis. The concentrations of Ca, P, and Si were determined by inductively coupled plasma-atomic emission spectrometry (ICP-AES; Varian Co., USA), and the pH values were measured using an electrolyte-type pH meter (Leici Co., Shanghai, China). The concentrations of Ca, P, and Si were measured as a function of the immersion time.

3 Results and discussion

3.1 Mechanical property of the composites

Tensile properties of PDLLA, PDLLA/BG, and PDLLA/KBG composites were analyzed by performing stress–strain experiments at 25°C. Figures 1 and 2 reveal the relationship between filler-volume fraction of the composites, the Young's modulus, and the tensile strength of the composites. The composite moduli increase with increasing BG content, as was expected, because of the

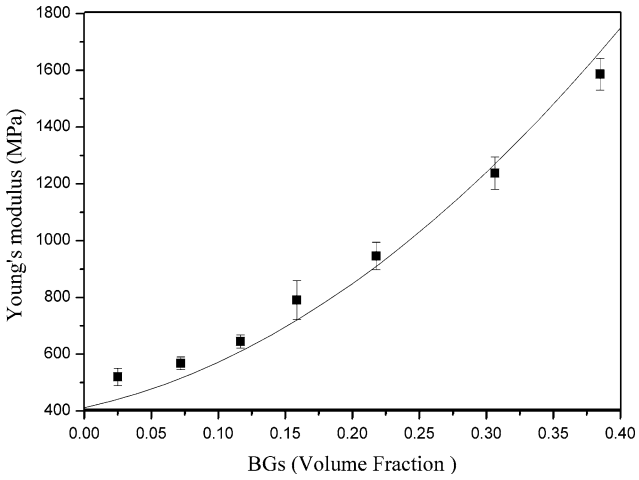

Fig. 1 Comparison of experimental data with theoretical predictions of Young's modulus for PDLLA/BG composites with respect to BG content. *Filled squares*-experimental values

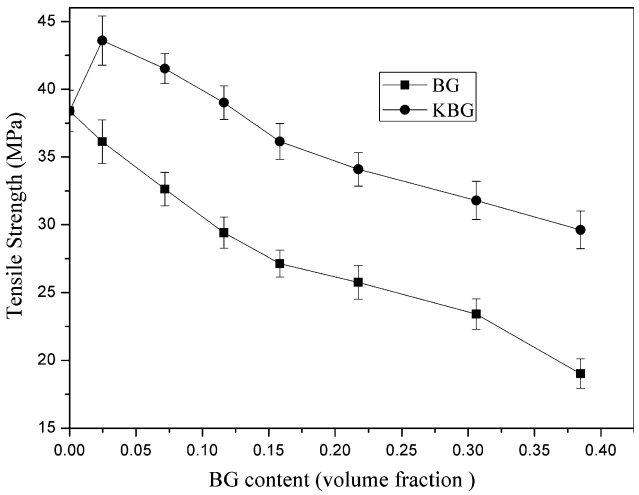

Fig. 2 Tensile strength of the PDLLA/BG and PDLLA/KBG composites with respect to BG content

stiffness of BG. The observed increase in the modulus of the BG-reinforced PDLLA can be explained in terms of the reinforcement effect.

The Young's modulus data for two-phase PDLLA/BG and PDLLA/KBG composites were compared with theoretical values that had been used to investigate the adhesion between a spherical filler and an incompressible matrix [29]. In order to evaluate the affinity between the polymer matrix (PDLLA) and BG particles, the tensile data points obtained were compared with the predicted values using two classical models. Equation 1 is Einstein's viscosity equation as modified by Guth and Gold [30].

$$E_c = E_p\left(1 + 2.5V_f + 14.1V_f^2\right) \quad (1)$$

where E_c and E_p are the moduli of the composite and polymer matrix, while V_f is the volume fraction of the filler

in the composite. Using this equation, we obtained a straight line (Fig. 1), which indicates that the predicted values are considerably in accordance with the experimental ones. The KBG particles did not make the remarkable difference in Young's modulus at a lower given particle content. This is because the Young's modulus is measured at small deformation.

Figure 2 shows the association between the tensile strength of PDLLA/BG and PDLLA/KBG composites and their filler content, i.e., BG and KBG. The higher the KBG content, the larger the difference between them because the tensile strength of the PDLLA/BG composites decreased more rapidly with the filler content than that of PDLLA/KBG composites. Nonetheless, the incorporation of KBG into the PDLLA matrix results in higher tensile strength compared with the incorporation of unmodified BG. As shown in Fig. 2, the decrease in the tensile strength is less obvious for the composites where the surface of BG particles was treated with a silane-coupling agent. This could possibly be due to a stronger interactivity between the filler/matrix interface in the PDLLA/KBG composites than in the PDLLA/BG composites.

In order to determine the extent of the interfacial interactions, the following equation derived by Pukanszky [31] was used:

$$\sigma_{yc} = \sigma_{yp}\frac{1 - V_f}{1 + 2.5V_f}\exp(BV_f) \quad (2)$$

Here, σ_{yc} and σ_{yp} are the yield stresses of the composite and the matrix, respectively, V_f is the volume fraction of the filler BG, and B is a parameter that characterizes the interfacial interactions in the composite. The surface area of the filler, the properties of the interphase, surface treatment, aggregation, and the matrix properties influence the strength of the composites and thus the value of parameter B [31, 32]. Generally, a higher value of interaction parameter B indicates stronger interfacial interactions [31]. For defining parameter B in the PDLLA/BG and PDLLA/KBG composites, $\ln\left[\left(\sigma_{yc}(1 + 2.5V_f)\right)/\left(\sigma_{yp}(1 - V_f)\right)\right]$ was plotted against V_f. The slopes of the straight lines obtained in the plot depict the values of the interaction parameter B; these values have been listed in Table 1. The higher value of the interaction parameter B in Table 1 confirms higher interfacial interactions between the PDLLA matrix and KBG. The value of the interaction parameter B for the PDLLA/KBG composites is higher compared to that for the PDLLA/BG composites, thus implying that the latter composites have stronger interfacial interactions.

Table 1 Interaction parameter B for the PDLLA/BG and PDLLA/KBG composites

Composites	B
PDLLA/BG	1.23
PDLLA/KBG	1.41

The change in tensile strength and interaction parameter B was mainly because of the greater aggregation of BG particles in the composite with higher filler content. The composites containing BG and KBG particles exhibit a rougher surface than those without fillers (Fig. 3). This could be due to the agglomeration of the particles in the matrix. The pure PDLLA samples were flat, smooth, and had a non-porous surface with no evidence of surface irregularity, as observed during the SEM analysis (Fig. 3). On the other hand, PDLLA/BG composites displayed a markedly different topography (Fig. 3). These samples exhibited an even distribution of BG particles, with few agglomerates, which were covered by the PDLLA matrix. The BG particles protruded from the surface, and there were gaps between each particle. The composite filled with BG particles had a rougher surface compared to the pure PDLLA films. However, in the PDLLA/KBG films, the KBG particles were uniformly distributed in the PDLLA matrix; hence, the PDLLA/KBG films had a slicker surface compared to the PDLLA/BG films.

The variations in the tensile strength of the composites with varying filler content showed that the surface modification of particles played an important role in defining the properties of the composite. After surface modification, the compatibility between KBG particles and the PDLLA matrix could be improved such that the particles could be dispersed more easily and homogeneously in the PDLLA matrix. The modified surface of the BG particles could enhance the binding of these particles to the PDLLA, and hence, the phase separation between the particles and the PDLLA matrix could be partially prevented.

3.2 In vitro bioactivity studies in SBF

Variations in the surface properties of the PDLLA/BG and PDLLA/KBG composites (22% vol). and pure PDLLA before and after soaking in SBF were analyzed using XRD and SEM. Figure 4 shows the XRD patterns of the pure PDLLA film before immersion and after 7, 14, and 21 days of incubation in SBF; the patterns indicate that it has an amorphous structure before immersion, while there are no apatite formations on its surface after immersion. However, the XRD patterns of the composites containing BG and KBG particles demonstrated the formation of HAP after immersion in SBF for 21 days, as shown in Fig. 4.

After the surface-modified films were immersed for 7 days in SBF, small crystals developed on the surface of the composite specimens in regions close to the BG particles. It can be observed that the apatite-like round particles are formed and there is a clear boundary between

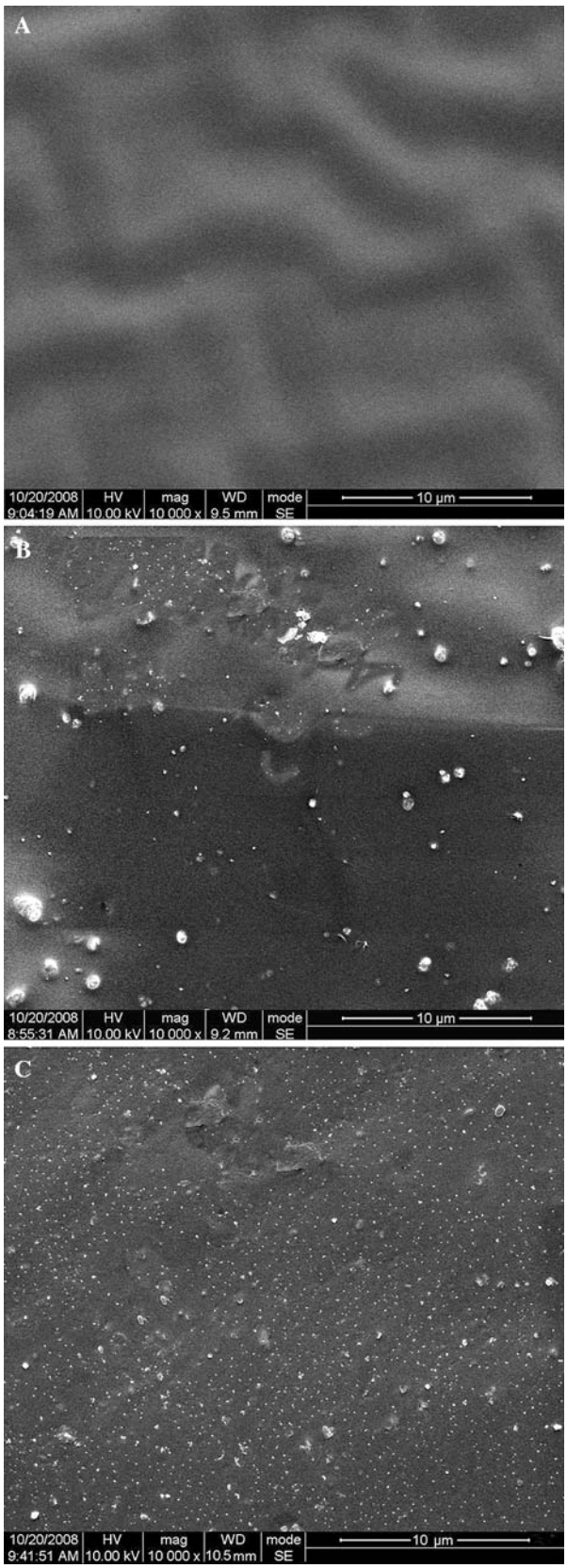

Fig. 3 SEM micrographs of the tensile fracture surfaces of **a** pure PDLLA, **b** PDLLA/BG, and **c** PDLLA/KBG composites

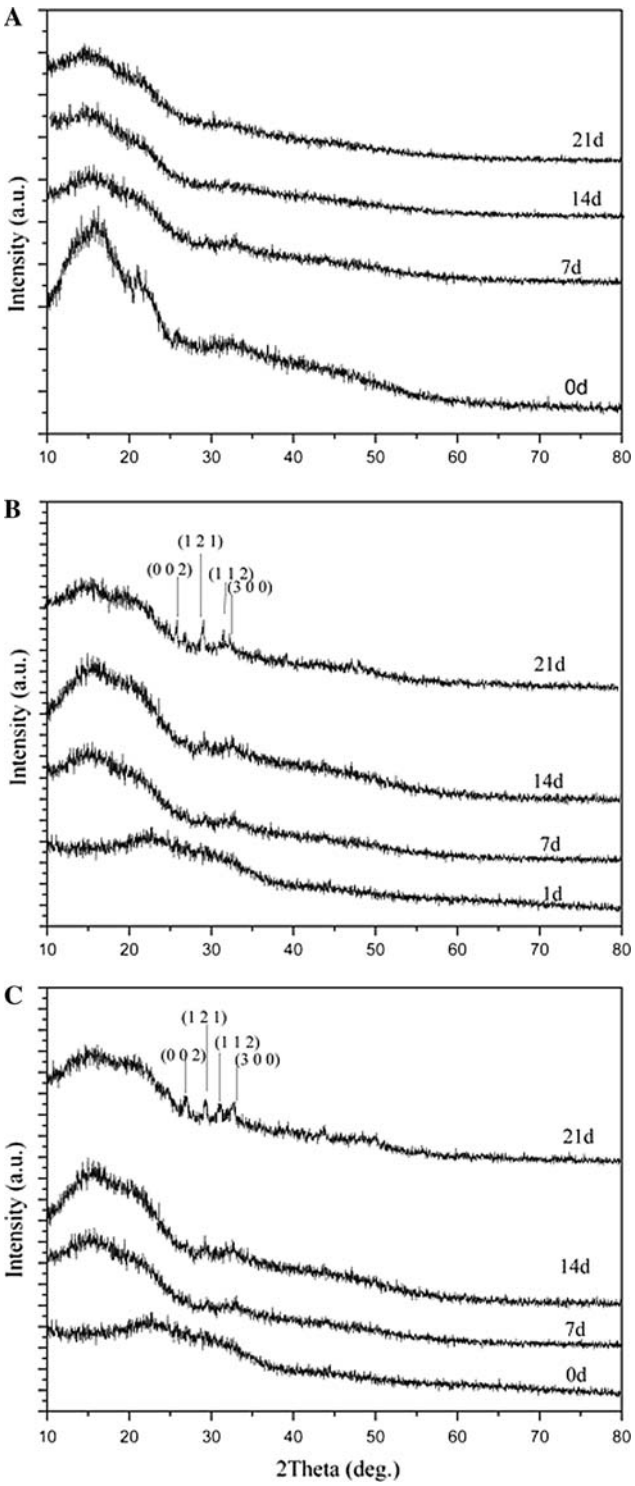

Fig. 4 XRD pattern of **a** pure PDLLA, **b** PDLLA/BG, and **c** PDLLA/KBG composites after incubation periods of 7, 14, and 21 days in SBF solution

adjacent particles; this confirmed that HAP particles always grow from BG agglomerates in the samples (Fig. 5). It was also observed that the round apatite-like

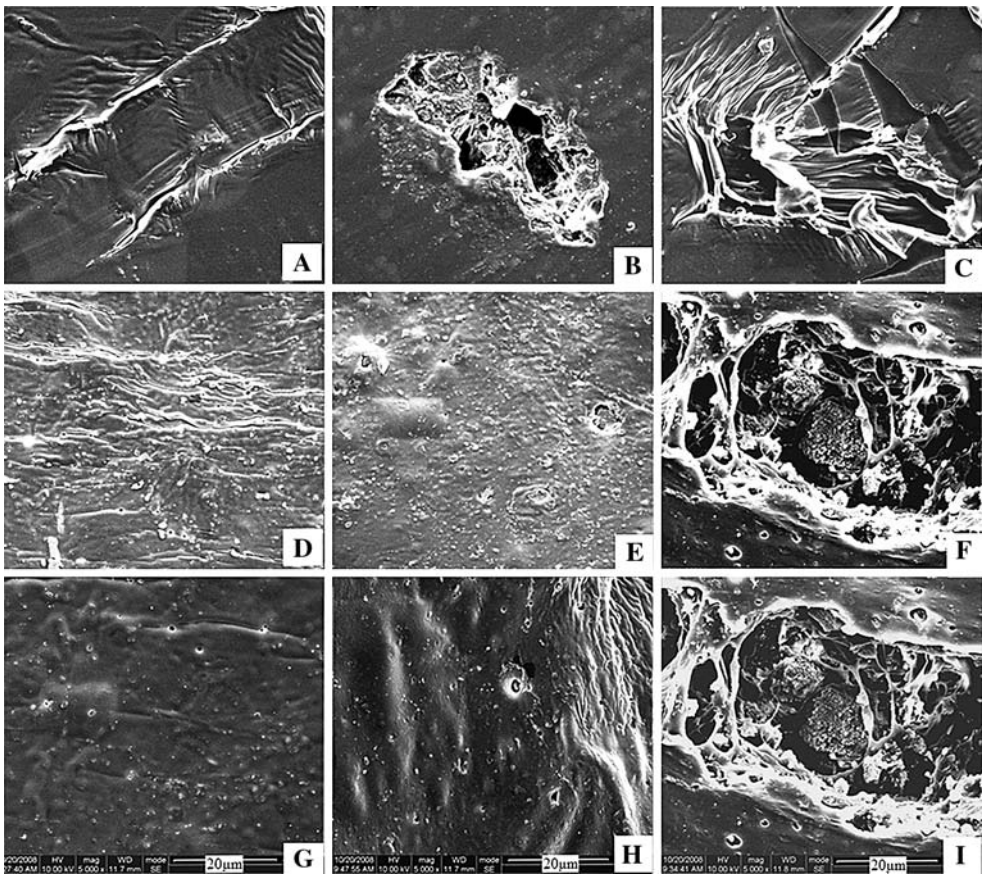

Fig. 5 SEM micrographs of pure PDLLA (**a**, **b**, and **c**), PDLLA/BG (**d**, **e**, and **f**), and PDLLA/KBG (**g**, **h**, and **i**) composites after incubation periods of 7, 14, and 21 days in SBF solution, respectively

particles were not distributed homogeneously throughout the film surface. However, the HAP formation on the PDLLA/KBG films was more homogeneous throughout the surface than that on the PDLLA/BG films. This was because the KBG particles were uniformly distributed in the PDLLA matrix. Even after immersion of the PDLLA/KBG films for 21 days in SBF, there was no apparent change in the surface microstructure and roughness of the films.

3.3 The changes in ionic concentration in SBF

Figure 6a shows the ICP-AES results of soluble extracts prepared with composites PDLLA/BG (22 vol%) after immersion in SBF. It was observed that the concentration of silicon increases initially, reaches a maximum at 3 days, and then decreases. This finding indicates that Si is initially released during the dissolution of BG particles in SBF and subsequently develops into an amorphous silica layer on the sample surface. Moreover, Fig. 6 shows that the concentrations of calcium and phosphorous decrease with increasing immersion time in SBF, which indicates that a HAP layer is being formed on the composite surfaces, as anticipated. The silica hydroxide (Si–OH) groups that form in the presence of calcium ions, disassociating from the BG particles react with water molecules; this leads to a negatively charged composite surfaces. The positively charged calcium ions are attracted to the composite surfaces, resulting in the formation of calcium phosphate. The hydrated silica on the surface of the BG particles provides favorable sites for apatite nucleation; this is the "classical theory of bioactivity" that was proposed by Hench [12, 13].

Figure 6b shows the temporal changes in pH that were observed during the immersion time. For pure PDLLA, the pH slightly decreased from 7.4 to 6.9 for the first 21 days. However, for the PDLLA/BG and PDLLA/KBG composites, a more rapid increase in pH (7.4–7.65) was observed for the first 7 days. The results obtained in the present study indicated that both PDLLA/BG and PDLLA/KBG composites could compensate for the decrease in the pH of the SBF solution. Compared to pure PDLLA, the PDLLA/BG and PDLLA/KBG composites maintained the pH of the media in the physiological range throughout the test periods. The dissolution of alkaline ions from the BG particles locally countered the acidification of the SBF due to the formation of acidic products by PDLLA degradation.

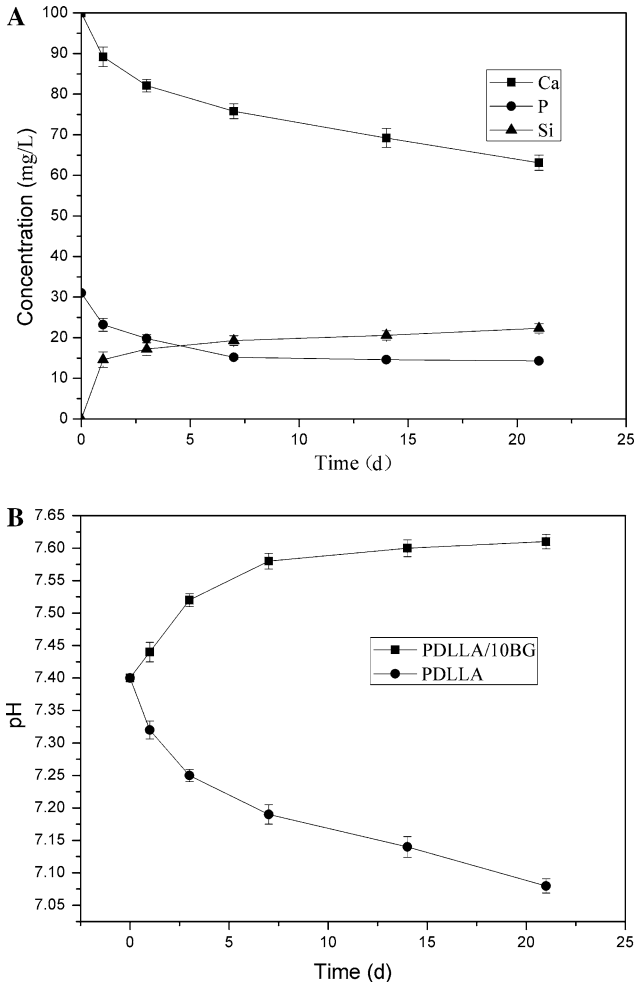

Fig. 6 Changes in the SBF solution induced by the immersion of the composites as a function of immersion time, **a** changes in ionic concentrations of Ca, P, and Si and **b** changes in pH

The composites containing BG and KBG had shown the bioactivity as is shown in XRD pattern (Fig. 4) and SEM micrographs (Fig. 5). Besides, there is no difference between PDLLA/BG and PDLLA/KBG in the changes of ionic concentration and pH in the SBF solution. So in the ICP-AES graph, only one kind of the composites containing BG can show the changes in the SBF solution induced by the immersion of the composites containing particles.

4 Conclusion

In order to improve the phase compatibility between the polymer and inorganic phase, the silane-coupling agent 3-glycidoxypropyltrimethoxysilane (KH570) was used to modify the surface of BG particles. PDLLA/KBG and PDLLA/BG composites were prepared by the solution-mixing method. The Young's modulus of the composite foams could be predicted by using an approach based on the models developed by Guth and Gold. The improvement in the interfacial interaction was confirmed by using a semiempirical equation developed by Pukanszky. The Paukanszky modulus showed that the interaction parameter B of PDLLA/KBG composites were higher than that of the PDLLA/BG composites; this shows that the interfacial interaction between the PDLLA matrix and KBG was higher. Stronger interfacial interactions in the PDLLA/KBG composites indicated that these composites had higher tensile strength than the PDLLA/BG composites. The modified BG particles could be dispersed uniformly in the composites; hence, the PDLLA/KBG composites had greater tensile strength than the PDLLA/BG composites or pure PDLLA when the filling content was low. Composites containing KBG were better incorporated into the PDLLA matrix. Treatment with the silane-coupling agent enhanced the mechanical properties of the composites in comparison with the composites containing non-treated BG particles. At a low content (~5 vol%) of KBG, the PDLLA/KBG composites exhibited higher tensile strength. The addition of BG enhanced the Young's modulus but decreased the tensile strength of the composites. At a higher content (e.g., 20 vol%), the modulus was remarkably increased. The improved mechanical property showed that the composites can be used non-load bearing bone repair. All of these results indicated that the composites PDLLA/KBG and PDLLA/BG showed obviously bioactive property through adding KBG and BG to PDLLA. The potential bone-bonding ability of the composites was demonstrated by the development of bone-like apatite on the surfaces of the composites after soaking them in SBF.

References

1. Wu L, Ding J. In vitro degradation of three-dimensional porous poly(D,L-lactide-co-glycolide) scaffolds for tissue engineering. Biomaterials. 2004;25:5821–30. doi:10.1016/j.biomaterials.2004.01.038.
2. Lin ASP, Barrows TH, Cartmell SH, Guldberg RE. Microarchitectural and mechanical characterization of oriented porous polymer scaffolds. Biomaterials. 2003;24:481–91. doi:10.1016/S0142-9612(02)00361-7.
3. Reed AM, Gilding DK. Biodegradable polymers for use in surgery-Poly(glycolic)/poly(lactic acid) homo and copolymers: 2. In vitro degradation. Polymer. 1981;22:494–8. doi:10.1016/0032-3861(81)90168-3.
4. Cai Q, Yang J, Bei J, Wang S. A novel porous cells scaffold made of polylactide–dextran blend by combining phase-separation and particle-leaching techniques. Biomaterials. 2002;23:4483–92. doi:10.1016/S0142-9612(02)00168-0.
5. Yoon SN, Yoon JJ, Park TG. A novel fabrication method of macroporous biodegradable polymer scaffolds using gas foaming salt as a porogen additive. J Biomed Mater Res B Appl Biomater. 2000;53:1–7.
6. Leenstra TS, Maltha JC, Kuijpers-Jagtman AM. Biodegradation of non-porous films after submucoperiosteal implantation on the palate of beagle dogs. J Mater Sci Mater Med. 1995;6:445–50.

7. Wang HT, Palmer H, Linhardt RJ, Flanagan DR, Schmitt E. Degradation of poly(ester) microspheres. Biomaterials. 1990;11:679–85. doi:10.1016/0142-9612(90)90026-M.
8. Mikos AG, Thorsen AJ, Czerwonka LA, Yuan B, Langer R, Winslow DN, et al. Preparation and characterization of poly(l-lactic acid) foams. Polymer. 1994;35:1068–77. doi:10.1016/0032-3861(94)90953-9.
9. Schugens C, Maquet V, Grandfils C, Jerome R, Teyssie P. Biodegradable and macroporous polylactide implants for cell transplantation: 1. Preparation of macroporous polylactide supports by solid-liquid phase separation. Polymer (Guildf). 1996;37:1027–38. doi:10.1016/0032-3861(96)87287-9.
10. Schugens C, Maquet V, Grandfils C, Jerome R, Teyssie P. Biodegradable and macroporous polylactide implants for cell transplantation. Polylactide macroporous biodegradable implants for cell transplantation. II. Preparation of polylactide foams by liquid-liquid phase separation. J Biomed Mater Res. 1996;30:449–61. doi:10.1002/(SICI)1097-4636(199604)30:4<449::AID-JBM3>3.0.CO;2-P.
11. Agrawal CM, Ray RB. Biodegradable polymeric scaffolds for musculoskeletal tissue engineering. J Biomed Mater Res. 2001;55:141–50. doi:10.1002/1097-4636(200105)55:2<141::AID-JBM1000>3.0.CO;2-J.
12. Hench LL. Bioceramics. J Am Ceram Soc. 1998;81:1705–28.
13. Hench LL. Bioceramics: from concept to clinic. J Am Ceram Soc. 1991;74:1487–510. doi:10.1111/j.1151-2916.1991.tb07132.x.
14. Hench LL, Splinter RJ, Allen WC, Greenlee TK. Bonding mechanisms at the interface of ceramic prosthetic materials. J Biomed Mater Res Symp. 1971;2:117–41.
15. Kokubo T, Kushitani H, Sakka S, Kitsugi T, Yamamum T. Solutions able to reproduce in vivo surface-structure changes in bioactive glass-ceramic A-W^3. J Biomed Mater Res Symp. 1990;24:721–34.
16. Hench LL, Julia MP. Third-Generation Biomedical Materials. Science. 2002;295:1014–7. doi:10.1126/science.1067404.
17. Porter AE, Thian ES, Huang J. Bioceramics: past, present, and for the future. J Eur Ceram Soc. 1992;3:145–50.
18. Gheysen G, Ducheyne P, Hench LL, De Meester P. Bioglass composites—A potential material for dental application. Biomaterials. 1983;4:81–4. doi:10.1016/0142-9612(83)90044-3.
19. Kokubo T. Bioactive glass ceramics: properties and applications. Biomatenals. 1991;12:155–63. doi:10.1016/0142-9612(91)90194-F.
20. Maria AL, Fernando JM, Jose DS. Glass–reinforced hydroxyapatite composites: fracture toughness and hardness dependence on microstructrural charateristics. Biomatenals. 1999;20:2085–90.
21. Christopher JD, Russell PJ. Bone graft and bone graft substitutes: A review of current technology and applications. J Appl Biomater. 1991;2:187–208. doi:10.1002/jab.770020307.
22. Gentleman E, Julia MP. Historic and current strategies in bone tissue engineering: Do we have a hope in Hench? J Mater Sci Mater Med. 2006;17:1029–35. doi:10.1007/s10856-006-0440-z.
23. Yang Y, Zhang H, Wang P, Zheng Q, Li J. The influence of nano-sized TiO2 fillers on the morphologies and properties of PSF UF membrane. J Membr Sci. 2007;288:231–8. doi:10.1016/j.memsci.2006.11.019.
24. Khoa NP, Damian F, Kwesi S-C. Surface modification for stability of nano-sized silica colloids. J Colloid Interface Sci. 2007;315:123–7. doi:10.1016/j.jcis.2007.06.064.
25. Hong Z, Zhang P, Liu A, Chen L, Chen X, Jing X. Composites of poly(lactide-co-glycolide) and the surface modified carbonated hydroxyapatite nanoparticles. J Biomed Mater Res A. 2007;81A:515–22. doi:10.1002/jbm.a.31038.
26. Liu A, Hong Z, Zhuang X, Chen X, Cui Y, Liu Y, et al. Surface modification of bioactive glass nanoparticles and the mechanical and biological properties of poly(l-lactide) composites. Acta Biomater. 2008;4:1005–15. doi:10.1016/j.actbio.2008.02.013.
27. Ramila A, Balas F, Vallet-Regf M. Synthesis routes for bioactive sol–gel glasses: alkoxides versus nitrates. Chem Mater. 2002;14:542–8. doi:10.1021/cm0110876.
28. Metin D, Tihminlioglu F, Balkose D, Ulku S. The effect of interfacial interactions on the mechanical properties of polypropylene/natural zeolite composites. Compos Part A. 2004;35:23–32. doi:10.1016/j.compositesa.2003.09.021.
29. Fu S, Feng X, Lauke B, Mai Y. Effects of particle size, particle/matrix interface adhesion and particle loading on mechanical properties of particulate–polymer composites. Compos Part B Eng. 2008;39(6):933–61.
30. Evelin DB, Chris CW, Montgomery TS. Mechanical properties of blends of HDPE and recycled urea-formaldehyde resin. J Appl Polym Sci. 2000;77:3220–7. doi:10.1002/1097-4628(20000929)77:14<3220::AID-APP250>3.0.CO;2-4.
31. Pukanszky B. Influence of interface interaction on the ultimate tensile properties of polymer composites. Composites. 1990;21:255–62. doi:10.1016/0010-4361(90)90240-W.
32. Masouras K, Akhtar R, Watts DC, Silikas N. Effect of filler size and shape on local nanoindentation modulus of resin-composites. J Mater Sci Mater Med. 2008;19:3561–6. doi:10.1007/s10856-008-3520-4.